Eur. Phys. J. C 18, 601–612 (2001)
Digital Object Identifier (DOI) 10.1007/s100520100556

THE EUROPEAN PHYSICAL JOURNAL C

Renormalization of Wilson operators in the light-cone gauge

A. Andraši[a]

"Rudjer Bošković" Institute, Zagreb, Croatia

Received: 31 May 2000 / Published online: 23 January 2001 – © Springer-Verlag 2001

Abstract. We test the renormalization of Wilson operators and the Mandelstam–Leibbrandt gauge in the case when the sides of the loop are parallel to the n, n^* vectors used in the M–L gauge. Graphs which in the Feynman gauge are free of ultra-violet divergences, in the M–L gauge show double divergences and single divergences with non-local Si and Ci functions. These non-local functions cancel out when we add all graphs together and the constraints of gauge invariance are satisfied. In Appendix C we briefly discuss the problems of the M–L gauge for loops containing spacelike lines.

1. Introduction

The aim of this research is to test the Mandelstam–Leibbrandt gauge, which is the best form of the lightcone gauge with the condition $n \cdot A = 0$, $n^2 = 0$ (where n is a vector used to define the gauge).

The Wilson operator is defined as

$$W = \mathrm{Tr} P \exp\left(-\mathrm{i}g \int_C A \cdot \mathrm{d}x\right), \tag{1}$$

where C is a closed curve, P denotes operator and matrix ordering along C, and the non-abelian gauge field A_μ is a matrix in some representation R of the gauge group G. The path-ordered phase factors (1) are gauge-invariant objects and therefore an ideal laboratory for testing different gauges. Also they are better coordinates in a non-abelian theory than are the conventional vector gauge field matrices $A_\mu(x)$, even though they are functions of all closed paths. The gauge-variant gauge fields greatly overdescribe the observable dynamics. The operators (1) are in contrast gauge-invariant, more precisely describe the dynamics and satisfy gauge-invariant equations. The hope has therefore arisen that the $W's$ can replace the $A's$ as fundamental dynamical variables, and correspondingly that the loop functions (Wilson operators) can replace the Green's functions.

However, the loop functions are perturbatively even more divergent than the Green's functions [1]. Therefore, to make any sense out of the above program, one must renormalize. This has already been done in Lorentz gauges [2,3]. In this paper we discuss the renormalization of Wilson operators in the Mandelstam–Leibbrandt light-cone gauge which became popular with the revival and intensive research of string theories. The complexity of the explicit calculations of individual graphs to order g^4 is a hint to the usefulness of the light-cone gauge in perturbative QCD for itself. Apart from that, in Appendix C we explain why strict application of dimensional regularization in the light-cone gauge is not possible in the case of spacelike and/or timelike lines.

It was noted [1] that if the Wilson loop contains a straight lightlike segment, charge renormalization does not work in a simple graph-by-graph way, but does work when certain graphs are added together. In the M–L gauge, renormalization is even more complicated. We shall show to order g^4 in perturbation theory that W in the M–L gauge obeys multiplicative renormalizability as required in [1],

$$W_{\mathrm{R}}(A_{\mathrm{R}}; g_{\mathrm{R}}) = Z(\epsilon) W_{\mathrm{B}}(A_{\mathrm{B}}; g_{\mathrm{B}}, \epsilon), \tag{2}$$

where the suffices R and B denote renormalized and bare quantities, and dimensional regularization with $d = 4 - \epsilon$ is used. The relationship between g_{B} and g_{R} and between A_{R} and A_{B} should be the same as in ordinary perturbation theory. $Z(\epsilon)$ is determined from the vacuum expectation value $\langle W \rangle$

$$\langle W_{\mathrm{R}}(g_{\mathrm{R}}) \rangle = Z(\epsilon) \langle W_{\mathrm{B}}(g_{\mathrm{B}}, \epsilon) \rangle. \tag{3}$$

However, the divergences of the individual graphs are not of the short distance nature and are non-local on the curve C. They are grouped into four tensors $n^*_\beta n^*_\rho$, $n_\beta n^*_\rho$, $n^*_\beta n_\rho$ and $n_\beta n_\rho$. There are no transverse divergences of the type e.g. $n_\beta P_\rho$, $P_\beta P_\rho$ (we use the decomposition of the momentum $p_\rho = (1/2) n^*_\rho p_+ + (1/2) n_\rho p_- + P_\rho$), nor $g_{\beta\rho}$ divergences, as argued in Appendix A.

Let the divergent part of the amplitude for the emission of two real gluons in momentum space be

$$M_{\beta\rho} = A n_\beta n_\rho + B n_\beta n^*_\rho + C n^*_\beta n_\rho + D n^*_\beta n^*_\rho,$$

where M is the coefficient of the two fields when we expand W in terms of the fields, and n and n^* are the lightlike vectors used to define the gluon propagator in the M–L gauge

$$G_{\beta\rho} = (k^2 + \mathrm{i}\eta) \left\{ -g_{\beta\rho} + \frac{n_\beta k_\rho + n_\rho k_\beta}{n \cdot k + \mathrm{i}\omega n^* \cdot k} \right\}. \tag{4}$$

[a] e-mail: andrasi@thphys.irb.hr

The polarization vectors should satisfy

$$p \cdot e = 0, \quad q \cdot f = 0,$$

and can be chosen to satisfy

$$n \cdot e = n \cdot f = 0,$$

e.g.

$$e_\beta = \frac{p_+ n^*_\beta - p_- n_\beta - 2p_\beta}{|4p_+p_-|^{1/2}},$$
$$f_\rho = \frac{q_+ n^*_\rho - q_- n_\rho - 2q_\rho}{|4q_+q_-|^{1/2}}, \tag{5}$$

for p and q on shell, respectively. The other independent polarization vector which is perpendicular to P, n and n^* and counterpart to e, gives zero when contracted into $M_{\beta\rho}$ and so plays no role in this paper. Of course, there is a counterpart of f as well.

We have four identities following from gauge invariance, which the amplitude should satisfy.

(a) $M^{\beta\rho} e_\beta f_\rho$ should be the same as the Feynman gauge when the external momenta p and q are on shell,
(b) $M^{\beta\rho} e_\beta q_\rho = 0$ for p on shell, $M^{\beta\rho} p_\beta f_\rho = 0$ for q on shell,
(c)

$$M^{\beta\rho} p_\beta q_\rho = 0. \tag{6}$$

These equations allow us to redefine the vectors (5) by

$$e'_\beta = p_- n_\beta - p_+ n^*_\beta,$$
$$f'_\rho = q_- n_\rho - q_+ n^*_\rho,$$

and the tensor structure (4) which satisfies (b) and (c) can be written in the form

$$M_{\beta\rho} = e'_\beta f'_\rho M. \tag{7}$$

The form (7) will in Sect. 5 be crucial to show that non-local divergences must cancel. (a), (b) and (c) impose the constraint on (4) of

$$p_+q_+A + p_+q_-B - p_-q_+C - p_-q_-D = 0,$$
$$p_+q_+A - p_+q_-B + q_+p_-C - p_-q_-D = 0,$$
$$p_+q_+A + p_+q_-B + p_-q_+C + p_-q_-D = 0,$$

i.e.

$$q_+A + q_-B = 0, \tag{8}$$

and fix all the ratios of $A : B : C : D$. The answers that we find in (15), (22) and (32) confirm this prediction and are invariant under $n \to cn$, $n^* \to cn^*$, $p_+ \to cp_+$, $p_- \to cp_-$ for any constant c.

A, B, C and D turn out to be local, although from the example of the self-energy graph [4], one might have expected non-local divergences to occur with the Wilson loop. If we take a self-energy part and try to derive an on-shell physical entity, we get zero (we take $S_{\beta\rho}(p)$, put $p^2 = 0$, multiply by $e_\beta e_\rho$ where e is a polarization vector satisfying $p \cdot e = 0$). Therefore, we cannot deduce much by arguing that physical things are gauge-invariant – we get just $0 = 0$. But, for the Wilson loop, we *do not* get zero if we put $p^2 = q^2 = 0$ and multiply by polarization vectors. So the gauge-independence argument does give some information. As the Feynman gauge non-local divergences cancel [1], (a), (b) and (c) explain why there are no non-local divergences in the M–L Wilson operator.

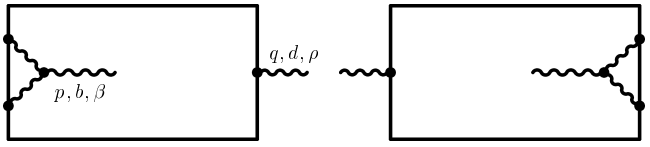

Fig. 1. Wilson operator at order g^4 with two real gluons and one 3-gluon vertex. The sides of the loop are along the lightlike vectors used to define the M–L prescription, n^* of length L and n of length T. The two graphs of the A-set which contribute to the n^*n^* sector have their symmetric counterparts

The abelian $C_\mathrm{R}C_\mathrm{R}$ part obeys the factorization theorem [5,6]. Therefore in this work we shall concentrate only on the non-abelian $C_\mathrm{G}C_\mathrm{R}$ part of the graphs, where C_R and C_G are the Casimirs for the representation used to define the Wilson loop and the gluons. In the following sections we list final results for the amplitude $M_{\beta\rho}$ to order g^4 after the decomposition in (4). The graphs are grouped into sets according to their topological equivalence.

2. The $n^*_\beta n^*_\rho$ sector of W_B

We list the final results for groups of graphs shown in the figures. The multiplication by the overall factor $C_{\beta\rho}$ is understood for each graph.

$$M_{\beta\rho} = C_{\beta\rho} M,$$

$$C_{\beta\rho} = \frac{2}{\epsilon} g^4 C_\mathrm{G} \mathrm{Tr}(t_b t_d) n^*_\beta n^*_\rho \pi^{2-(\epsilon/2)} (2\pi)^{-n}.$$

We denote the frequent non-local functions which appear in all equations by

$$\mathrm{Ci}(x) = \int_0^x \frac{\cos t - 1}{t} \mathrm{d}t,$$
$$\mathrm{Si}(x) = \int_0^x \frac{\sin t}{t} \mathrm{d}t. \tag{9}$$

A-set

The graphs contributing to the A-set are shown in Fig. 1. There are also graphs with p and q interchanged. Then the ultra-violet divergent part of the graphs in Fig. 1 is

$$(M_1 + M_2)(\mathrm{A}) = -\frac{1}{p_-q_-} (\mathrm{e}^{-\mathrm{i}p_+T} + \mathrm{e}^{-\mathrm{i}q_+T})(\mathrm{e}^{-\mathrm{i}q_-L} - 1)$$

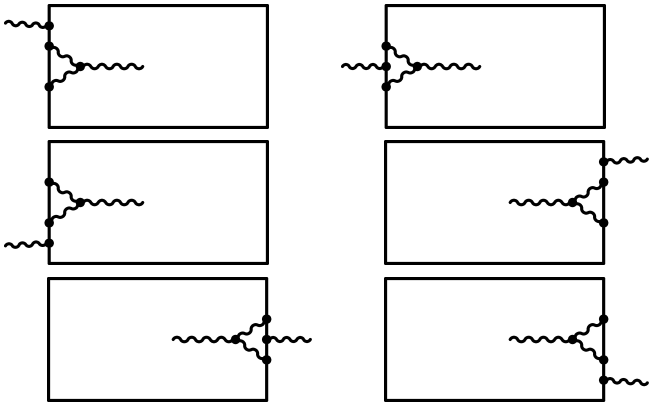

Fig. 2. B-set of graphs

$$\times\{2(\mathrm{e}^{-\mathrm{i}p_-L}-1)+(\mathrm{e}^{-\mathrm{i}p_-L}-1)\mathrm{Ci}(p_-L)$$
$$+\mathrm{i}(\mathrm{e}^{-\mathrm{i}p_-L}+1)\mathrm{Si}(p_-L)\}. \qquad (10)$$

B-set

The B-graphs are shown in Fig. 2. Addition of symmetric graphs is understood.

$$\begin{aligned}
&(M_1+M_2+...+M_6)(\mathrm{B})=(\mathrm{e}^{-\mathrm{i}\mathrm{Tr}+}+1)\\
&\times\left\{\frac{2}{p_-q_-}(\mathrm{e}^{-\mathrm{i}p_-L}-1)(\mathrm{e}^{-\mathrm{i}q_-L}-1)+\left(\frac{2}{p_-q_-}+\frac{2}{p_-r_-}\right)\right.\\
&\times[(\mathrm{e}^{-\mathrm{i}r_-L}+1)\mathrm{Ci}(r_-L)+\mathrm{i}(\mathrm{e}^{-\mathrm{i}r_-L}-1)\mathrm{Si}(r_-L)]\\
&-\left(\frac{2}{p_-q_-}+\frac{2}{p_-r_-}\right)\\
&\times[(\mathrm{e}^{-\mathrm{i}r_-L}+1)\mathrm{Ci}(q_-L)+\mathrm{i}(\mathrm{e}^{-\mathrm{i}r_-L}-1)\mathrm{Si}(q_-L)]\\
&-\left(\frac{2}{p_-r_-}\right)\\
&\times[(\mathrm{e}^{-\mathrm{i}r_-L}+1)\mathrm{Ci}(p_-L)+\mathrm{i}(\mathrm{e}^{-\mathrm{i}r_-L}-1)\mathrm{Si}(p_-L)]\\
&-\left(\frac{1}{p_-q_-}\right)\\
&\times(\mathrm{e}^{-\mathrm{i}q_-L}+1)[(\mathrm{e}^{-\mathrm{i}p_-L}+1)\mathrm{Ci}(p_-L)\\
&\left.+\mathrm{i}(\mathrm{e}^{-\mathrm{i}p_-L}-1)\mathrm{Si}(p_-L)]\right\}
\end{aligned}$$

where

$$r=p+q. \qquad (11)$$

C-set

The C-graphs are shown in Fig. 3.

$$\begin{aligned}
&(M_1+M_2+M_3+M_4)(\mathrm{C})=\frac{2}{q_-r_-}(\mathrm{e}^{-\mathrm{i}Tp_+}+\mathrm{e}^{-\mathrm{i}Tq_+})\\
&\times\{(\mathrm{e}^{-\mathrm{i}r_-L}+1)\\
&\times[\mathrm{Ci}(q_-L)-\mathrm{Ci}(p_-L)]+\mathrm{i}(\mathrm{e}^{-\mathrm{i}r_-L}-1)
\end{aligned}$$

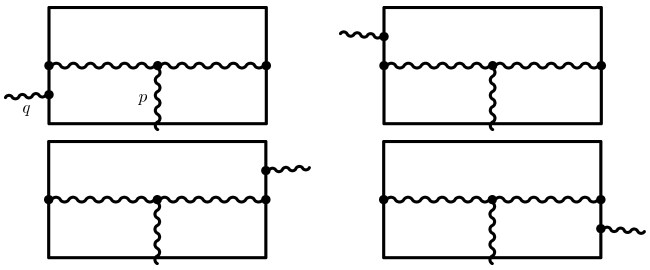

Fig. 3. C-set

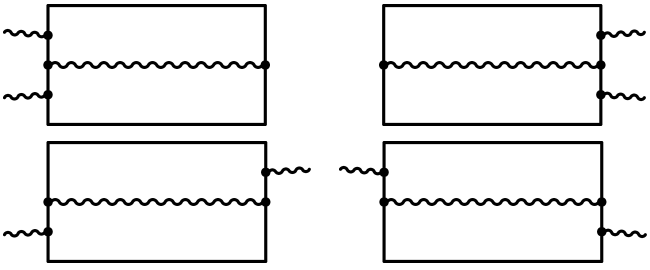

Fig. 4. D-set

$$\begin{aligned}
&\times[\mathrm{Si}(q_-L)-\mathrm{Si}(p_-L)]\}\\
&+\frac{2}{q_-r_-}(\mathrm{e}^{-\mathrm{i}\mathrm{Tr}+}+1)\\
&\times[(\mathrm{e}^{-\mathrm{i}r_-L}+1)\mathrm{Ci}(r_-L)+\mathrm{i}(\mathrm{e}^{-\mathrm{i}r_-L}-1)\mathrm{Si}(r_-L)]\\
&-\frac{1}{q_-p_-}(\mathrm{e}^{-\mathrm{i}Tp_+}-1)(\mathrm{e}^{-\mathrm{i}Tq_+}-1)(\mathrm{e}^{-\mathrm{i}Lq_-}+1)\\
&\times[(\mathrm{e}^{-\mathrm{i}p_-L}+1)\mathrm{Ci}(p_-L)+\mathrm{i}(\mathrm{e}^{-\mathrm{i}p_-L}-1)\mathrm{Si}(p_-L)]\\
&+\left(\frac{\mathrm{i}\pi}{p_-q_-}\right)\\
&\times(\mathrm{e}^{-\mathrm{i}Tp_+}+1)(\mathrm{e}^{-\mathrm{i}Tq_+}-1)(\mathrm{e}^{-\mathrm{i}p_-L}-1)(\mathrm{e}^{-\mathrm{i}q_-L}+1)\\
&-\left(\frac{2\mathrm{i}\pi}{q_-r_-}\right)\\
&\times(\mathrm{e}^{-\mathrm{i}Tp_+}+1)(\mathrm{e}^{-\mathrm{i}Tq_+}-1)(\mathrm{e}^{-\mathrm{i}r_-L}-1). \qquad (12)
\end{aligned}$$

Again we have to add the symmetric graphs with p and q interchanged.

D-set

The complete set of D-graphs (including symmetric graphs) is shown in Fig. 4.

$$\begin{aligned}
&(M_1+M_2+...+M_8)(\mathrm{D})=-\frac{2}{p_-q_-}(\mathrm{e}^{-\mathrm{i}\mathrm{Tr}+}+1)\\
&\times\{2(\mathrm{e}^{-\mathrm{i}r_-L}+1)\mathrm{Ci}(r_-L)+2\mathrm{i}(\mathrm{e}^{-\mathrm{i}r_-L}-1)\mathrm{Si}(r_-L)\\
&-(\mathrm{e}^{-\mathrm{i}p_-L}+1)\\
&\times[(\mathrm{e}^{-\mathrm{i}q_-L}+1)\mathrm{Ci}(q_-L)+\mathrm{i}(\mathrm{e}^{-\mathrm{i}q_-L}-1)\mathrm{Si}(q_-L)]\\
&-(\mathrm{e}^{-\mathrm{i}q_-L}+1)\\
&\times[(\mathrm{e}^{-\mathrm{i}p_-L}+1)\mathrm{Ci}(p_-L)+\mathrm{i}(\mathrm{e}^{-\mathrm{i}p_-L}-1)\mathrm{Si}(p_-L)]\}\\
&-2\left(\frac{1}{q_-r_-}-\frac{1}{p_-r_-}\right)(\mathrm{e}^{-\mathrm{i}Tp_+}+\mathrm{e}^{-\mathrm{i}Tq_+})
\end{aligned}$$

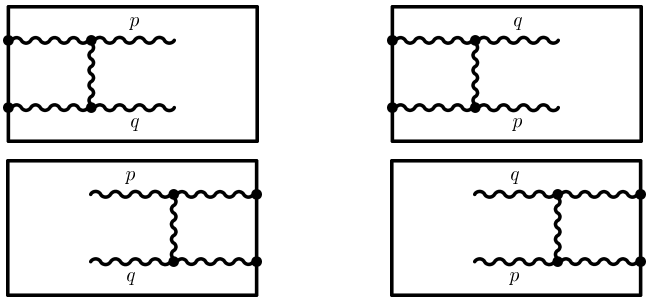

Fig. 5. E-set

$$
\begin{aligned}
&\times\{(\mathrm{e}^{-\mathrm{i}r_-L}+1)[\mathrm{Ci}(q_-L)-\mathrm{Ci}(p_-L)]\\
&+\mathrm{i}(\mathrm{e}^{-\mathrm{i}r_-L}-1)[\mathrm{Si}(q_-L)-\mathrm{Si}(p_-L)]\}\\
&-\frac{2}{p_-q_-}(\mathrm{e}^{-\mathrm{i}Tp_+}+\mathrm{e}^{-\mathrm{i}Tq_+})\\
&\times[(\mathrm{e}^{-\mathrm{i}q_-L}+1)\mathrm{Ci}(q_-L)+\mathrm{i}(\mathrm{e}^{-\mathrm{i}q_-L}-1)\mathrm{Si}(q_-L)]\\
&-\frac{2}{p_-q_-}(\mathrm{e}^{-\mathrm{i}Tp_+}+\mathrm{e}^{-\mathrm{i}Tq_+})\\
&\times[(\mathrm{e}^{-\mathrm{i}p_-L}+1)\mathrm{Ci}(p_-L)+\mathrm{i}(\mathrm{e}^{-\mathrm{i}p_-L}-1)\mathrm{Si}(p_-L)]\\
&-\frac{2}{p_-q_-}(\mathrm{e}^{-\mathrm{i}Tp_+}+\mathrm{e}^{-\mathrm{i}Tq_+})(\mathrm{e}^{-\mathrm{i}p_-L}-1)\\
&\times[\mathrm{Ci}(q_-L)-\mathrm{iSi}(q_-L)]\\
&-\frac{2}{p_-q_-}(\mathrm{e}^{-\mathrm{i}Tp_+}+\mathrm{e}^{-\mathrm{i}Tq_+})(\mathrm{e}^{-\mathrm{i}q_-L}-1)\\
&\times[\mathrm{Ci}(p_-L)-\mathrm{iSi}(p_-L)]\\
&-\frac{2\mathrm{i}\pi}{p_-q_-}(\mathrm{e}^{-\mathrm{i}Tp_+}-\mathrm{e}^{-\mathrm{i}Tq_+})(\mathrm{e}^{-\mathrm{i}q_-L}-\mathrm{e}^{-\mathrm{i}p_-L})\\
&-2\mathrm{i}\pi\left(\frac{1}{p_-r_-}-\frac{1}{q_-r_-}\right)\\
&\times(\mathrm{e}^{-\mathrm{i}r_-L}-1)(\mathrm{e}^{-\mathrm{i}Tq_+}-\mathrm{e}^{-\mathrm{i}Tp_+}). \qquad (13)
\end{aligned}
$$

E-set

The E-set is shown in Fig. 5.

$$
\begin{aligned}
&(M_1+\ldots+M_4)(\mathrm{E})=-4(\mathrm{e}^{-\mathrm{i}\mathrm{Tr}_+}+1)\\
&\times\left\{\left(\frac{1}{p_-q_-}\right)\right.\\
&\times[(\mathrm{e}^{-\mathrm{i}r_-L}+1)\mathrm{Ci}(r_-L)+\mathrm{i}(\mathrm{e}^{-\mathrm{i}r_-L}-1)\mathrm{Si}(r_-L)]\\
&-\left(\frac{1}{q_-r_-}\right)\\
&\times[(\mathrm{e}^{-\mathrm{i}r_-L}+1)\mathrm{Ci}(p_-L)+\mathrm{i}(\mathrm{e}^{-\mathrm{i}r_-L}-1)\mathrm{Si}(p_-L)]\\
&-\left(\frac{1}{p_-r_-}\right)\\
&\left.\times\,[(\mathrm{e}^{-\mathrm{i}r_-L}+1)\mathrm{Ci}(q_-L)+\mathrm{i}(\mathrm{e}^{-\mathrm{i}r_-L}-1)\mathrm{Si}(q_-L)]\right\}. \qquad (14)
\end{aligned}
$$

The complete sum of all the graphs contributing to the n^*n^* sector is very simple:

$$
S_{\beta\rho}(n^*n^*)=\frac{8}{\epsilon}g^4C_\mathrm{G}\mathrm{Tr}(t_bt_d)n^*_\beta n^*_\rho\pi^{2-(\epsilon/2)}(2\pi)^{-4}
$$

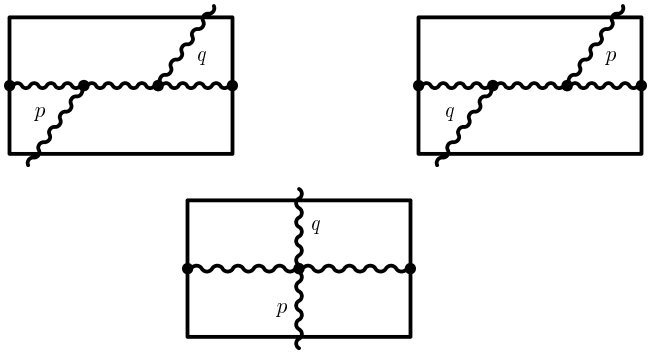

Fig. 6. Graphs with two 3-gluon vertices and a graph with the 4-gluon vertex which contribute to the nn sector of the Wilson operator at order g^4

$$
\begin{aligned}
&\times\frac{1}{p_-q_-}(\mathrm{e}^{-\mathrm{i}Tq_+}-1)(\mathrm{e}^{-\mathrm{i}Tp_+}-1)\\
&\times(\mathrm{e}^{-\mathrm{i}q_-L}-1)(\mathrm{e}^{-\mathrm{i}p_-L}-1)\\
&=\frac{8}{\epsilon}g^2C_\mathrm{G}\pi^2(2\pi)^{-4}B_{\beta\rho}(n^*n^*), \qquad (15)
\end{aligned}
$$

where $B_{\beta\rho}(n^*n^*)$ denotes the Born term which is in the n^*n^* sector only. The non-local functions have cancelled. This result alone does not prove renormalizability as the field renormalization matrix in the lightcone gauge mixes all three sectors.

3. The $n_\beta n_\rho$ sector of W_B

Again we list the final results, but here the overall factor is

$$
\begin{aligned}
&C'_{\beta\rho}=\frac{2}{\epsilon}g^4C_\mathrm{G}\mathrm{Tr}(t_bt_d)n_\beta n_\rho\pi^{2-(\epsilon/2)}(2\pi)^{-n}\frac{1}{q_+p_+},\\
&M_{\beta\rho}=C'_{\beta\rho}M. \qquad (16)
\end{aligned}
$$

G2-set

The sum of the three graphs of the G2-set shown in Fig. 6 is

$$
\begin{aligned}
&M(\mathrm{G2})=-\frac{8}{\epsilon}(\mathrm{e}^{-\mathrm{i}r_-L}+1)(\mathrm{e}^{-\mathrm{i}Tp_+}-1)(\mathrm{e}^{-\mathrm{i}Tq_+}-1)\\
&-2(\mathrm{e}^{-\mathrm{i}Tp_+}-1)(\mathrm{e}^{-\mathrm{i}Tq_+}-1)\{(\mathrm{e}^{-\mathrm{i}r_-L}+1)\\
&\times[\mathrm{Ci}(r_-L)+2\ln(TL\mu^2)+\mathrm{i}\pi]\\
&+\mathrm{i}(\mathrm{e}^{-\mathrm{i}r_-L}-1)\mathrm{Si}(r_-L)\}\\
&-2(\mathrm{e}^{-\mathrm{i}Tq_+}+\mathrm{e}^{-\mathrm{i}Tp_+})\{(\mathrm{e}^{-\mathrm{i}r_-L}+1)\\
&\times[\mathrm{Ci}(r_-L)-\mathrm{Ci}(q_-L)-\mathrm{Ci}(p_-L)]\\
&+\mathrm{i}(\mathrm{e}^{-\mathrm{i}r_-L}-1)\\
&\times[\mathrm{Si}(r_-L)-\mathrm{Si}(q_-L)-\mathrm{Si}(p_-L)]\}. \qquad (17)
\end{aligned}
$$

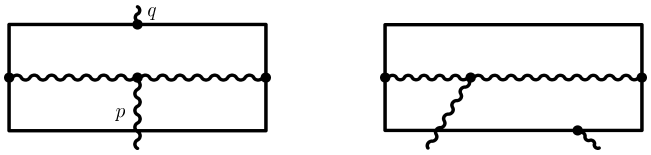

Fig. 7. G1-set of graphs. Graphs with one 3-gluon vertex which contribute to the nn sector

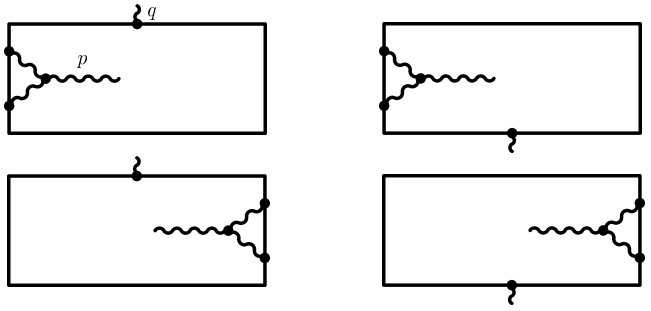

Fig. 8. Same as Fig. 7

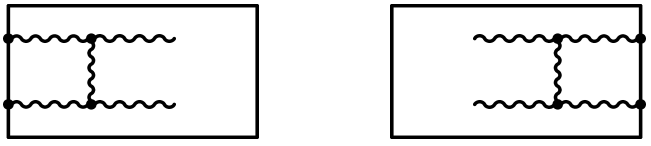

Fig. 9. Left and right graphs with two 3-gluon vertices in the G(L+R)-set which contribute to the nn sector

G1-set

The G1-set of graphs are the graphs with one 3-gluon vertex. There are two groups of such graphs. The two graphs shown in Fig. 7 give

$$\begin{aligned} M^a(\mathrm{G1}) &= (\mathrm{e}^{-\mathrm{i}Tp_+}-1)(\mathrm{e}^{-\mathrm{i}Tq_+}-1)(\mathrm{e}^{-\mathrm{i}q_-L}+1)\\ &\times\left\{(\mathrm{e}^{-\mathrm{i}p_-L}+1)\right.\\ &\times\left[\mathrm{Ci}(p_-L)+2\gamma+\frac{4}{\epsilon}+\mathrm{i}\pi+2\ln(TL\mu^2)\right]\\ &\left.+\,\mathrm{i}(\mathrm{e}^{-\mathrm{i}p_-L}-1)\mathrm{Si}(p_-L)\right\}. \end{aligned} \tag{18}$$

Of course the graphs with p and q interchanged must be added. The graphs in Fig. 8 give

$$\begin{aligned} M^b(\mathrm{G1}) &= (\mathrm{e}^{-\mathrm{i}Tp_+}-1)(\mathrm{e}^{-\mathrm{i}Tq_+}-1)(\mathrm{e}^{-\mathrm{i}q_-L}-1)\\ &\times\{2(\mathrm{e}^{-\mathrm{i}p_-L}-1)+(\mathrm{e}^{-\mathrm{i}p_-L}-1)\mathrm{Ci}(p_-L)\\ &+\mathrm{i}(\mathrm{e}^{-\mathrm{i}p_-L}+1)\mathrm{Si}(p_-L)\}. \end{aligned} \tag{19}$$

Again there is a symmetric set of graphs with p and q interchanged.

G(L+R)-set

Adding the symmetric graphs to Fig. 9, the total sum of the four graphs is

$$\begin{aligned} M(\mathrm{G(L+R)}) &= -2(\mathrm{e}^{-\mathrm{i}\mathrm{Tr}_+}+1)\{(\mathrm{e}^{-\mathrm{i}r_-L}+1)\\ &\times[\mathrm{Ci}(p_-L)+\mathrm{Ci}(q_-L)-\mathrm{Ci}(r_-L)]\\ &+\mathrm{i}(\mathrm{e}^{-\mathrm{i}r_-L}-1)\\ &\times[\mathrm{Si}(p_-L)+\mathrm{Si}(q_-L)-\mathrm{Si}(r_-L)]\}. \end{aligned} \tag{20}$$

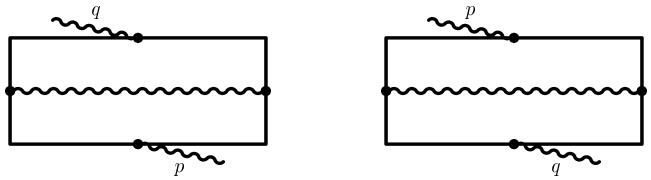

Fig. 10. G0-set of graphs in the nn sector

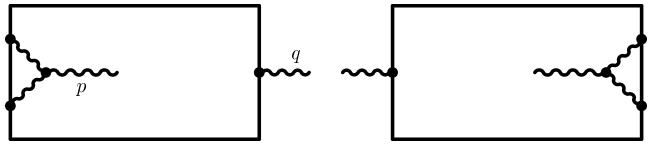

Fig. 11. The A-set of graphs which contribute to the $n_\beta n^*_\rho$ sector

G0-set

Figure 10 gives

$$\begin{aligned} M(\mathrm{G0}) &= -\frac{8}{\epsilon}(\mathrm{e}^{-\mathrm{i}Tp_+}-1)(\mathrm{e}^{-\mathrm{i}Tq_+}-1)(\mathrm{e}^{-\mathrm{i}q_-L}+\mathrm{e}^{-\mathrm{i}p_-L})\\ &\times(\mu^2TL)^{\epsilon/2}\left(1+\gamma\frac{\epsilon}{2}+\frac{\mathrm{i}\pi\epsilon}{4}\right). \end{aligned} \tag{21}$$

The sum of all the graphs contributing to the nn sector is

$$\begin{aligned} S_{\beta\rho}(nn) &= \frac{8}{\epsilon}(\mathrm{e}^{-\mathrm{i}Tp_+}-1)(\mathrm{e}^{-\mathrm{i}Tq_+}-1)\\ &\times(\mathrm{e}^{-\mathrm{i}p_-L}-1)(\mathrm{e}^{-\mathrm{i}q_-L}-1)\left(\frac{1}{q_+p_+}\right)\\ &\times g^4C_\mathrm{G}\mathrm{Tr}(t_bt_d)n_\beta n_\rho\pi^{2-(\epsilon/2)}(2\pi)^{-4}\\ &=\frac{8}{\epsilon}g^2C_\mathrm{G}\pi^2(2\pi)^{-4}B_{\beta\rho}(nn), \end{aligned} \tag{22}$$

where $B_{\beta\rho}(nn)$ is the g^2 term for the nn sector of W_B (g_B,ϵ).

4. The $n_\beta n^*_\rho$ sector of W_B

The final results for the $n_\rho n^*_\beta$ sector we get from $n_\beta n^*_\rho$ by the change p,b,β into q,d,ρ. The overall factor for all the graphs in this sector is

$$\begin{aligned} C''_{\beta\rho} &= \frac{2}{\epsilon}g^4C_\mathrm{G}\mathrm{Tr}(t_bt_d)n_\beta n^*_\rho\pi^{2-(\epsilon/2)}(2\pi)^{-n},\\ M_{\beta\rho} &= C''_{\beta\rho}M. \end{aligned} \tag{23}$$

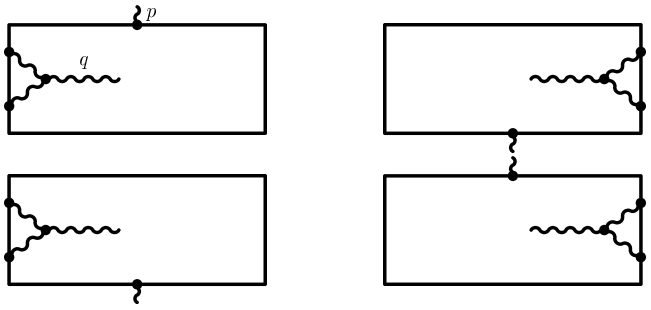

Fig. 12. The A′-set of graphs

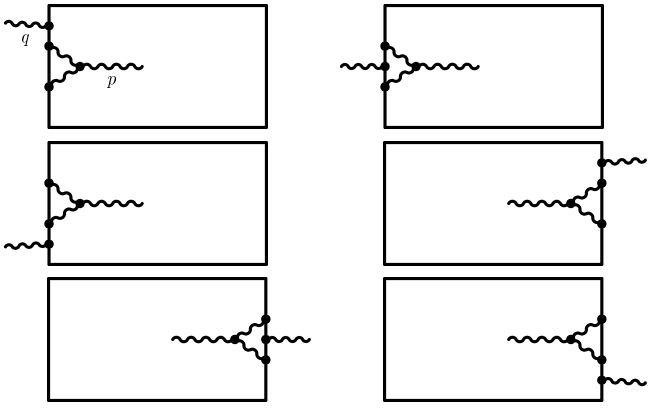

Fig. 13. B-set of graphs in the $n_\beta n^*_\rho$ sector

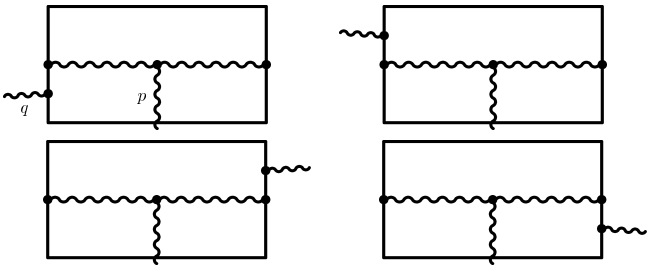

Fig. 14. C-set of graphs

A-set

The graphs in Fig. 11 give

$$
\begin{aligned}
M(\mathrm{A}) = {} & (\mathrm{e}^{-\mathrm{i}Tq_+} + \mathrm{e}^{-\mathrm{i}Tp_+})(\mathrm{e}^{-\mathrm{i}q_-L} - 1)\left(\frac{1}{p_+q_-}\right) \\
& \times \{2(\mathrm{e}^{-\mathrm{i}p_-L} - 1) + (\mathrm{e}^{-\mathrm{i}p_-L} - 1)\mathrm{Ci}(p_-L) \\
& + \mathrm{i}(\mathrm{e}^{-\mathrm{i}p_-L} + 1)\mathrm{Si}(p_-L)\}. \qquad (24)
\end{aligned}
$$

A′-set

The A′-set is presented in Fig. 12.

$$
\begin{aligned}
M(\mathrm{A}') = {} & -(\mathrm{e}^{-\mathrm{i}Tp_+} - 1)(\mathrm{e}^{-\mathrm{i}Tq_+} - 1) \\
& \times (\mathrm{e}^{-\mathrm{i}p_-L} - 1)\left(\frac{1}{p_+q_-}\right) \\
& \times \left\{2(\mathrm{e}^{-\mathrm{i}q_-L} - 1) + (\mathrm{e}^{-\mathrm{i}q_-L} - 1)\mathrm{Ci}(q_-L)\right. \\
& \left. + \mathrm{i}(\mathrm{e}^{-\mathrm{i}q_-L} + 1)\mathrm{Si}(q_-L)\right\}. \qquad (25)
\end{aligned}
$$

B-set

The B-set is shown in Fig. 13.

$$
\begin{aligned}
M(\mathrm{B}) = {} & -(\mathrm{e}^{-\mathrm{i}\mathrm{Tr}_+} + 1)\left\{\frac{2}{p_+q_-}(\mathrm{e}^{-\mathrm{i}p_-L} - 1)(\mathrm{e}^{-\mathrm{i}q_-L} - 1)\right. \\
& + \left(\frac{2}{p_+q_-} + \frac{2}{p_+r_-}\right) \\
& \times [(\mathrm{e}^{-\mathrm{i}r_-L} + 1)\mathrm{Ci}(r_-L) + \mathrm{i}(\mathrm{e}^{-\mathrm{i}r_-L} - 1)\mathrm{Si}(r_-L)] \\
& - \left(\frac{2}{p_+q_-} + \frac{2}{p_+r_-}\right) \\
& \times [(\mathrm{e}^{-\mathrm{i}r_-L} + 1)\mathrm{Ci}(q_-L) + \mathrm{i}(\mathrm{e}^{-\mathrm{i}r_-L} - 1)\mathrm{Si}(q_-L)] \\
& + \left(\frac{2}{p_+r_-}\right) \\
& \times [(\mathrm{e}^{-\mathrm{i}r_-L} + 1)\mathrm{Ci}(p_-L) + \mathrm{i}(\mathrm{e}^{-\mathrm{i}r_-L} - 1)\mathrm{Si}(p_-L)] \\
& - \left(\frac{1}{p_+q_-}\right) \\
& \times (\mathrm{e}^{-\mathrm{i}q_-L} + 1)[(\mathrm{e}^{-\mathrm{i}p_-L} + 1)\mathrm{Ci}(p_-L) \\
& \left. + \mathrm{i}(\mathrm{e}^{-\mathrm{i}p_-L} - 1)\mathrm{Si}(p_-L)]\right\}. \qquad (26)
\end{aligned}
$$

C-set

Graphs grouped into the C-set are shown in Fig. 14.

$$
\begin{aligned}
M(\mathrm{C}) = {} & \frac{2}{p_+q_-}\left[\frac{2}{\epsilon} + \ln(TL\mu^2) + \gamma\right](\mathrm{e}^{-\mathrm{i}Tp_+} - 1) \\
& \times (\mathrm{e}^{-\mathrm{i}Tq_+} - 1)(\mathrm{e}^{-\mathrm{i}p_-L} - 1)(\mathrm{e}^{-\mathrm{i}q_-L} - 1) \\
& + 2(\mathrm{e}^{-\mathrm{i}\mathrm{Tr}_+} + 1)\left(\frac{1}{q_-p_+} + \frac{1}{r_-p_+}\right) \\
& \times \{(\mathrm{e}^{-\mathrm{i}r_-L} + 1)\mathrm{Ci}(r_-L) \\
& + \mathrm{i}(\mathrm{e}^{-\mathrm{i}r_-L} - 1)\mathrm{Si}(r_-L)\} \\
& - 2(\mathrm{e}^{-\mathrm{i}Tp_+} + \mathrm{e}^{-\mathrm{i}Tq_+})\left(\frac{1}{q_-p_+} + \frac{1}{r_-p_+}\right) \\
& \times \{(\mathrm{e}^{-\mathrm{i}r_-L} + 1)\mathrm{Ci}(q_-L) \\
& + \mathrm{i}(\mathrm{e}^{-\mathrm{i}r_-L} - 1)\mathrm{Si}(q_-L)\} \\
& + \left\{\frac{2}{r_-p_+}(\mathrm{e}^{-\mathrm{i}Tp_+} + \mathrm{e}^{-\mathrm{i}Tq_+})\right. \\
& - \frac{1}{q_-p_+}(\mathrm{e}^{-\mathrm{i}\mathrm{Tr}_+} + 1)(\mathrm{e}^{-\mathrm{i}q_-L} + 1) \\
& \left. + \frac{1}{q_-p_+}(\mathrm{e}^{-\mathrm{i}Tp_+} + \mathrm{e}^{-\mathrm{i}Tq_+})(\mathrm{e}^{-\mathrm{i}q_-L} - 1)\right\} \\
& \times \{\mathrm{Ci}(p_-L) - \mathrm{i}\mathrm{Si}(p_-L)\}
\end{aligned}
$$

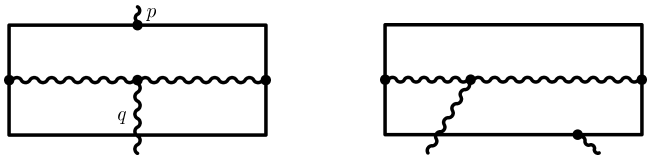

Fig. 15. C′-set

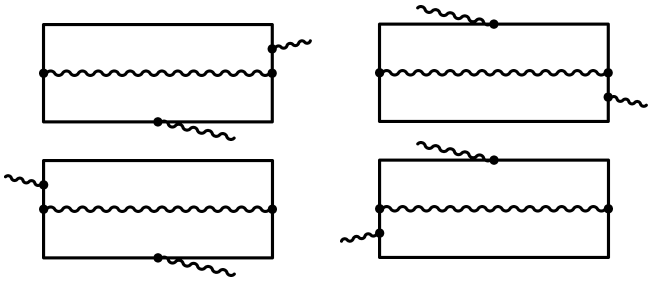

Fig. 16. D-set

$$
\begin{aligned}
&+\left\{\frac{2}{r_-p_+}\mathrm{e}^{-\mathrm{i}r_-L}(\mathrm{e}^{-\mathrm{i}Tp_+}+\mathrm{e}^{-\mathrm{i}Tq_+})\right.\\
&-\frac{1}{q_-p_+}\mathrm{e}^{-\mathrm{i}p_-L}(\mathrm{e}^{-\mathrm{i}q_-L}+1)(\mathrm{e}^{-\mathrm{i}\mathrm{Tr}_+}+1)\\
&\left.-\frac{1}{q_-p_+}\mathrm{e}^{-\mathrm{i}p_-L}(\mathrm{e}^{-\mathrm{i}q_-L}-1)(\mathrm{e}^{-\mathrm{i}Tp_+}+\mathrm{e}^{-\mathrm{i}Tq_+})\right\}\\
&\times\{\mathrm{Ci}(p_-L)+\mathrm{i}\mathrm{Si}(p_-L)\}\\
&+\frac{\mathrm{i}\pi}{q_-p_+}(\mathrm{e}^{-\mathrm{i}Tp_+}-1)(\mathrm{e}^{-\mathrm{i}Tq_+}-1)\\
&\times(\mathrm{e}^{-\mathrm{i}p_-L}-1)(\mathrm{e}^{-\mathrm{i}q_-L}-1)-\frac{2\mathrm{i}\pi}{r_-p_+}(\mathrm{e}^{-\mathrm{i}Tp_+}-1)\\
&\times(\mathrm{e}^{-\mathrm{i}Tq_+}+1)(\mathrm{e}^{-\mathrm{i}r_-L}-1). \qquad (27)
\end{aligned}
$$

C′-set

The two graphs of the C′-set in Fig. 15 give

$$
\begin{aligned}
M(\mathrm{C}') &= \frac{1}{q_-p_+}(\mathrm{e}^{-\mathrm{i}Tp_+}-1)(\mathrm{e}^{-\mathrm{i}p_-L}+1)\\
&\times\{(\mathrm{e}^{-\mathrm{i}Tq_+}-1)[(\mathrm{e}^{-\mathrm{i}q_-L}+1)\mathrm{Ci}(q_-L)\\
&+\mathrm{i}(\mathrm{e}^{-\mathrm{i}q_-L}-1)\mathrm{Si}(q_-L)]-3\mathrm{i}\pi(\mathrm{e}^{-\mathrm{i}q_-L}-1)\}. \qquad (28)
\end{aligned}
$$

D-set

The D-set is shown in Fig. 16.

$$
\begin{aligned}
M(\mathrm{D}) &= -\frac{2}{q_-p_+}\left[\frac{2}{\epsilon}+\ln(TL\mu^2)+\frac{\mathrm{i}\pi}{2}+\gamma\right]\\
&\times(\mathrm{e}^{-\mathrm{i}Tp_+}-1)(\mathrm{e}^{-\mathrm{i}Tq_+}-1)\\
&\times(\mathrm{e}^{-\mathrm{i}p_-L}-1)(\mathrm{e}^{-\mathrm{i}q_-L}-1)\\
&-\frac{2}{q_-p_+}(\mathrm{e}^{-\mathrm{i}Tp_+}-1)(\mathrm{e}^{-\mathrm{i}Tq_+}-1)(\mathrm{e}^{-\mathrm{i}p_-L}+1)
\end{aligned}
$$

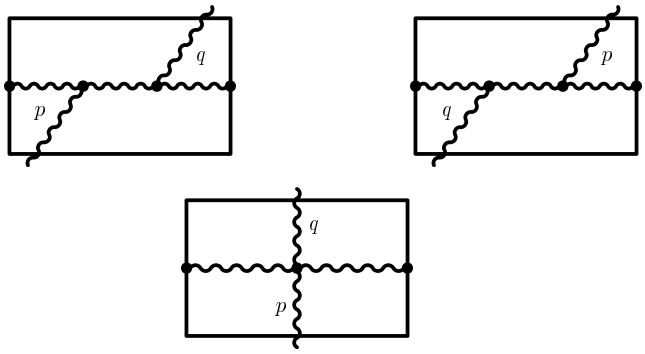

Fig. 17. E-set

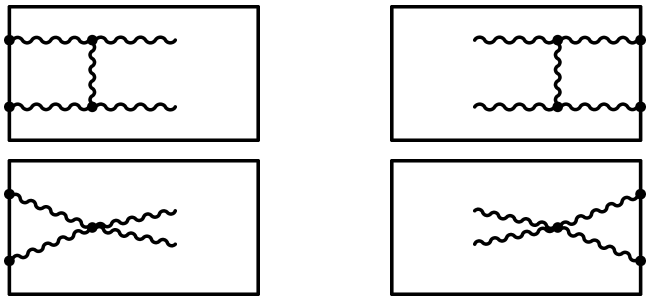

Fig. 18. F-set of graphs which contribute to the $n_\beta n_\rho^*$ sector

$$
\begin{aligned}
&\times\left\{(\mathrm{e}^{-\mathrm{i}q_-L}+1)\mathrm{Ci}(q_-L)\right.\\
&\left.+\mathrm{i}(\mathrm{e}^{-\mathrm{i}q_-L}-1)\left(\mathrm{Si}(q_-L)-\frac{\pi}{2}\right)\right\}+\frac{2\mathrm{i}\pi}{q_-p_+}\\
&\times(\mathrm{e}^{-\mathrm{i}Tp_+}-1)(\mathrm{e}^{-\mathrm{i}p_-L}+1)(\mathrm{e}^{-\mathrm{i}q_-L}-1). \qquad (29)
\end{aligned}
$$

E-set

The E-set contains graphs with two 3-gluon vertices and the graph with the 4-gluon vertex spanning across the loop. They are shown in Fig. 17.

$$
\begin{aligned}
M(\mathrm{E}) &= -\frac{2}{p_+r_-}\{(\mathrm{e}^{-\mathrm{i}\mathrm{Tr}_+}+1)\\
&\times[(\mathrm{e}^{-\mathrm{i}r_-L}+1)\mathrm{Ci}(r_-L)+\mathrm{i}(\mathrm{e}^{-\mathrm{i}r_-L}-1)\mathrm{Si}(r_-L)]\\
&+(\mathrm{e}^{-\mathrm{i}Tp_+}+\mathrm{e}^{-\mathrm{i}Tq_+})\\
&\times[(\mathrm{e}^{-\mathrm{i}r_-L}+1)(\mathrm{Ci}(p_-L)-\mathrm{Ci}(q_-L))\\
&+\mathrm{i}(\mathrm{e}^{-\mathrm{i}r_-L}-1)(\mathrm{Si}(p_-L)-\mathrm{Si}(q_-L))]\\
&-\mathrm{i}\pi(\mathrm{e}^{-\mathrm{i}r_-L}-1)(\mathrm{e}^{-\mathrm{i}Tq_+}+1)(\mathrm{e}^{-\mathrm{i}Tp_+}-1)\}. \qquad (30)
\end{aligned}
$$

F-set

The four graphs of the F-set are shown in Fig. 18. Of course, there are also symmetric graphs with p and q interchanged. The complete sum of eight graphs amounts to

$$
M(\mathrm{F}) = \frac{2}{p_+r_-}(\mathrm{e}^{-\mathrm{i}\mathrm{Tr}_+}+1)
$$

$$\times \{(\mathrm{e}^{-\mathrm{i}r_- L}+1)[\mathrm{Ci}(p_- L)-\mathrm{Ci}(q_- L)+\mathrm{Ci}(r_- L)] + \mathrm{i}(\mathrm{e}^{-\mathrm{i}r_- L}-1) \times [\mathrm{Si}(p_- L)-\mathrm{Si}(q_- L)+\mathrm{Si}(r_- L)]\}. \quad (31)$$

The total sum for the nn^* sector is

$$\begin{aligned} S_{\beta\rho}(nn^*) = &-\frac{8}{\epsilon} g^4 C_{\mathrm{G}} \mathrm{Tr}(t_b t_d) n_\beta n^*_\rho \pi^{2-(\epsilon/2)} (2\pi)^{-n} \\ &\times \frac{1}{p_+ q_-} (\mathrm{e}^{-\mathrm{i}Tp_+}-1)(\mathrm{e}^{-\mathrm{i}Tq_+}-1) \\ &\times (\mathrm{e}^{-\mathrm{i}p_- L}-1)(\mathrm{e}^{-\mathrm{i}q_- L}-1) \\ &-\frac{8}{\epsilon} g^4 C_{\mathrm{G}} \mathrm{Tr}(t_b t_d) n_\rho n^*_\beta \pi^{2-(\epsilon/2)} (2\pi)^{-n} \\ &\times \frac{1}{q_+ p_-} (\mathrm{e}^{-\mathrm{i}Tp_+}-1)(\mathrm{e}^{-\mathrm{i}Tq_+}-1) \\ &\times (\mathrm{e}^{-\mathrm{i}p_- L}-1)(\mathrm{e}^{-\mathrm{i}q_- L}-1). \end{aligned} \quad (32)$$

This is again proportional to the g^2 term with the same factor $8/\epsilon$ as in (15) and (22).

5. Discussion

We are now going to explain how (2) works out to order g^4. The field renormalization matrix in the M–L gauge is [8–10], in momentum space, where $A(p)$ is the gluon field in momentum space,

$$\begin{aligned} A^B_\beta(p) &= \left(1+\frac{11}{6}c\right) \\ &\times \left[g_{\beta\gamma} - c n_\beta (n^*_\gamma - \frac{n^*\cdot p}{n\cdot p + \mathrm{i}\eta n^*\cdot p} n_\gamma)\right] A^{\gamma R}(p) \\ &= z_{\beta\gamma} A^{\gamma R}(p), \end{aligned}$$

where

$$c = \frac{g^2_{\mathrm{R}}}{8\pi^2\epsilon} C_{\mathrm{G}},$$

and the coupling constant renormalization is

$$g_{\mathrm{B}} = \left(1-\frac{11}{6}c\right) g_{\mathrm{R}}. \quad (33)$$

On the right hand side (2) contains various sorts of fourth order terms:

(a) W_{B} to fourth order, Z, z and g_{B} to zeroth order;
(b) W_{B} to second order, Z to second order;
(c) W_{B} to second, g_{B} to second;
(d) W_{B} to second, z to second order.

Then (b) contributes only to the abelian $C_{\mathrm{R}}C_{\mathrm{R}}$ part, while (c) and (d) should give the counterterms needed to cancel the UV divergences we found in (a). Of course, since W_{B} to second order has two real gluons, that is two A_{B} operators, it gets two z factors, one depending on p and the other on q. We list counterterms for each sector separately.

(1) n^*n^* sector. Although the Born term is contained in the n^*n^* sector only, we had to study the off-shell sectors as well. The reason is the field renormalization matrix $z_{\beta\gamma}$ which mixes all three sectors. The Born term to order g^2 is

$$B_{\beta\rho}(n^*n^*) = \frac{1}{p_- q_-} g^2_{\mathrm{B}} n^*_\beta n^*_\rho H A^\beta_{\mathrm{B}}(p) A^\rho_{\mathrm{B}}(q),$$

where

$$\begin{aligned} H = &\mathrm{Tr}(t_b t_d)(\mathrm{e}^{-\mathrm{i}Tp_+}-1)(\mathrm{e}^{-\mathrm{i}Tq_+}-1) \\ &\times (\mathrm{e}^{-\mathrm{i}Lp_-}-1)(\mathrm{e}^{-\mathrm{i}Lq_-}-1). \end{aligned} \quad (34)$$

To order g^4_{R} the operator $(z-1)W_{\mathrm{B}} + (g_{\mathrm{B}}-g_{\mathrm{R}})W_{\mathrm{B}}$ on the right of (2) gives for the n^*n^* sector the counter-term

$$\begin{aligned} W^{ct}_{\beta\rho}(n^*n^*) = &\, n^*_\beta n^*_\rho \frac{g^2_{\mathrm{R}}}{p_- q_-} H \\ &\times \left[\frac{11}{6} c g^{\beta\gamma} - c n^\beta (n^{\gamma *} - \frac{n^*\cdot p}{n\cdot p} n^\gamma)\right] \\ &\times A^R_\gamma(p) A^R_\rho(q) \\ &+ n^*_\beta n^*_\rho \frac{g^2_{\mathrm{R}}}{p_- q_-} H \\ &\times \left[\frac{11}{6} c g^{\rho\gamma} - c n^\rho (n^{\gamma *} - \frac{n^*\cdot q}{n\cdot q} n^\gamma)\right] \\ &\times A^R_\gamma(q) A^R_\beta(p) \\ &- 2 n^*_\beta n^*_\rho \frac{11}{6} c H \frac{g^2_{\mathrm{R}}}{p_- q_-} A^{\beta R}(p) A^{\rho R}(q). \end{aligned} \quad (35)$$

We notice that the factor $(11/6)c$ cancels out between the wave function renormalization (two first terms) and the coupling constant renormalization (last term). Hence, the counter-term to order g^4_{R} for the n^*n^* sector is

$$\begin{aligned} W^{ct}_{\beta\rho}(n^*n^*) = &-4c n^*_\rho n^*_\beta \frac{1}{p_- q_-} H \\ &+ 2c[n^*_\beta n_\rho \frac{1}{p_- q_+} + n^*_\rho n_\beta \frac{1}{q_- p_+}] H. \end{aligned} \quad (36)$$

(2) nn^* sector.

$$\begin{aligned} W^{ct}_{\beta\rho}(nn^*) = &-4c n_\rho n_\beta \frac{1}{p_+ q_+} H \\ &+ 2c\left[n^*_\beta n_\rho \frac{1}{p_- q_+} + n^*_\rho n_\beta \frac{1}{p_+ q_-}\right] H. \end{aligned} \quad (37)$$

(3) nn sector gives zero. The sum of (1) and (2) gives exactly the counterterms needed to cancel (15), (22) and (32). The complications with non-local Si and Ci divergences were caused by the choice of the M–L gauge, not the lightlike sides of the Wilson loop, as shown in Appendix C. We certainly expected (a) of (6) to be gauge-invariant, but in fact we find that the *whole* of the divergent part of $M_{\beta\rho}$ is gauge-invariant.

We shall now explain how the field renormalization matrix $z_{\beta\gamma}$ leaves this tensor structure unchanged. Let us invoke the tensor structure for the amplitude in (7):

$$M_{\beta\rho} = e'_\beta f'_\rho M. \quad (38)$$

This vanishes when contracted with p_β or q_ρ. Then it is easy to see why $z_{\beta\gamma}$ does not change the structure. The non-local structure in $z_{\beta\gamma}$ contains

$$n_\beta\left(n^*_\gamma - \frac{n^*\cdot p}{n\cdot p}n_\gamma\right) = -\frac{n_\beta e'_\gamma}{p_+}. \tag{39}$$

When contracted with $M_{\beta\rho}$ the term $(n\cdot e')/p_+ = -2$ becomes free of non-localities.

Although we have demonstrated multiplicative renormalizability of Wilson operators to order g^4 in the M–L gauge, the complexity of the actual calculation raises the question of the usefulness of both, lightcone gauge and Wilson operators, as fundamental variables in perturbative QCD. The lightcone gauge has additional problems for loops containing spacelike and/or timelike lines as explained in Appendix C.

Acknowledgements. The author wishes to thank Prof. J.C. Taylor for the invaluable help and advice which made this work possible. The author is grateful to The Royal Society for financial help and D.A.M.T.P. for hospitality. This work was supported by the Ministry of Science and Technology of the Republic of Croatia under Contract No. 00980103.

Appendix A

There are no transverse components in the Wilson operator as we have assumed in (4). Let us take one of the characteristic integrals which appears in the graph with one 3-gluon vertex in Fig. 7.

$$\begin{aligned} Z_\beta &= \int \mathrm{d}^n k \frac{2K_\beta}{k^2(p-k)^2 k_+}(\mathrm{e}^{-\mathrm{i}T(p-k)_+} - \mathrm{e}^{-\mathrm{i}Tk_+}) \\ &\times \frac{1}{(p-k)_-}(\mathrm{e}^{-\mathrm{i}k_- L} - 1)(1 - e^{-\mathrm{i}(p-k)_- L}) \\ &= P_\beta \times M \end{aligned} \tag{A1}$$

We multiply both sides by the perpendicular momentum P_β, and write

$$\begin{aligned} 2P\cdot K &= K^2 - k_+k_- - (P-K)^2 + (p-k)_+(p-k)_- \\ &+ p_+k_- + p_-k_+, \end{aligned} \tag{A2}$$

$$\begin{aligned} Z\cdot P = P^2 \times M &= \int \mathrm{d}^n k \frac{(p-k)^2 - k^2 + p_-k_+ + p_+k_-}{k^2(p-k)^2k_+} \\ &\times \{\mathrm{e}^{-\mathrm{i}Tp_+}(\mathrm{e}^{\mathrm{i}Tk_+} - 1) \\ &- (\mathrm{e}^{-\mathrm{i}Tk_+} - 1) + (\mathrm{e}^{-\mathrm{i}Tp_+} - 1)\} \\ &\times \frac{1}{(p-k)_-} \\ &\times \{\mathrm{e}^{-\mathrm{i}p_- L}(\mathrm{e}^{\mathrm{i}(p-k)_- L} - 1) + \mathrm{e}^{-\mathrm{i}(p-k)_- L} - 1\}. \end{aligned} \tag{A3}$$

In this form we can integrate each of the terms in (A3). k_+p_- gives UV finite term as the integrals of the type

$$I = \int \mathrm{d}^n k \frac{1}{k^2(p-k)^2}\mathrm{e}^{\mathrm{i}Tk_+}\frac{1}{(p-k)_-}(\mathrm{e}^{-\mathrm{i}(p-k)_- L} - 1) \tag{A4}$$

contain the oscillating factor $\mathrm{e}^{\mathrm{i}Tk_+}$ which suppresses the possible UV divergences. Let us denote by Y the contribution from k_-p_+:

$$\begin{aligned} Y &= \int \mathrm{d}^n k \frac{p_+k_-}{k^2(p-k)^2k_+} \\ &\times \{\mathrm{e}^{-\mathrm{i}Tp_+}(\mathrm{e}^{\mathrm{i}Tk_+} - 1) - (\mathrm{e}^{-\mathrm{i}Tk_+} - 1) + (\mathrm{e}^{-\mathrm{i}Tp_+} - 1)\} \\ &\times \frac{1}{(p-k)_-} \\ &\times \{\mathrm{e}^{-\mathrm{i}p_- L}(\mathrm{e}^{\mathrm{i}(p-k)_- L} - 1) + \mathrm{e}^{-\mathrm{i}(p-k)_- L} - 1\}. \end{aligned} \tag{A5}$$

The factor $(\mathrm{e}^{-\mathrm{i}Tp_+} - 1)$ gives only a UV finite term. Also we can write

$$\frac{k_-}{(p-k)_-} = \frac{(k-p)_- + p_-}{(p-k)_-} = -1 \tag{A6}$$

modulo UV finite terms. We change the variable $p-k = k'$ and use the argument analogous to (A4) but now with k_+ and k_- interchanged. The integral

$$A = \int \mathrm{d}^n k \frac{1}{k^2(p-k)^2}\mathrm{e}^{\mathrm{i}k_- L}\frac{1}{(p-k)_+}(\mathrm{e}^{-\mathrm{i}(p-k)_+ T} - 1) \tag{A7}$$

is UV finite due to the oscillating factor $\mathrm{e}^{\mathrm{i}k_- L}$.

Therefore the UV divergent part of Y is

$$\begin{aligned} Y &= p_+(\mathrm{e}^{-\mathrm{i}p_- L} + 1)\int \mathrm{d}^n k \frac{1}{k^2(p-k)^2(p-k)_+} \\ &\times \{\mathrm{e}^{-\mathrm{i}Tp_+}(\mathrm{e}^{\mathrm{i}T(p-k)_+} - 1) - (\mathrm{e}^{-\mathrm{i}T(p-k)_+} - 1)\}. \end{aligned} \tag{A8}$$

After the integration over k_- using the formula

$$\begin{aligned} &\int \mathrm{d}^n k \frac{1}{k^2(p-k)^2} = \mathrm{i}\pi^{2-(\epsilon/2)}\Gamma\left(\frac{\epsilon}{2}\right)(-p^2 - \mathrm{i}\eta)^{-\epsilon/2} \\ &\times \int_0^1 \mathrm{d}x x^{-\epsilon/2}(1-x)^{-\epsilon/2}, \end{aligned}$$

where

$$k_+ = p_+x, \tag{A9}$$

we obtain

$$\begin{aligned} Y &= \mathrm{i}\pi^{2-(\epsilon/2)}\Gamma\left(\frac{\epsilon}{2}\right)(-p^2 - \mathrm{i}\eta)^{-\epsilon/2}(\mathrm{e}^{-\mathrm{i}p_- L} + 1) \\ &\times [(\mathrm{e}^{-\mathrm{i}Tp_+} - 1)\mathrm{Ci}(p_+T) + \mathrm{i}(\mathrm{e}^{-\mathrm{i}Tp_+} + 1) \\ &\times \mathrm{Si}(p_+T)]. \end{aligned} \tag{A10}$$

The remaining two integrals in (A3) we denote by E and F.

$$\begin{aligned} E &= \int \mathrm{d}^n k \frac{1}{k^2k_+} \\ &\times \{\mathrm{e}^{-\mathrm{i}Tp_+}(\mathrm{e}^{\mathrm{i}Tk_+} - 1) - (\mathrm{e}^{-\mathrm{i}Tk_+} - 1) + (\mathrm{e}^{-\mathrm{i}Tp_+} - 1)\} \\ &\times \left(\frac{1}{(p-k)_-}\right) \\ &\times \{\mathrm{e}^{-\mathrm{i}(p-k)_- L} - 1 + \mathrm{e}^{-\mathrm{i}p_- L}(\mathrm{e}^{\mathrm{i}(p-k)_- L} - 1)\}. \end{aligned} \tag{A11}$$

The term $(\mathrm{e}^{-\mathrm{i}Tp_+}-1)$ gives a vanishing contribution upon the integration in the complex k_+ plane:

$$\int \mathrm{d}^n k \frac{1}{k^2 k_+} f(p_-, k_-) = 0, \tag{A12}$$

because both poles lie in the same half plane with k_+ regulated in the sense of Mandelstam [7]. Other terms have no pole at $k_+ = 0$. For the first $(\mathrm{e}^{\mathrm{i}Tk_+}-1)$ we close the contour in the upper half plane and pick up a pole at $k_+ = ((K^2-\mathrm{i}\eta)/k_-)\theta(-k_-)$, while for the second $(\mathrm{e}^{-\mathrm{i}Tk_+}-1)$ we close the contour in the lower half plane and pick up a pole at $k_+ = ((K^2-\mathrm{i}\eta)/k_-)\theta(k_-)$.

$$\begin{aligned} E = {} & \mathrm{i}\pi \mathrm{e}^{-\mathrm{i}Tp_+} \int_{-\infty}^{0} \mathrm{d}k_- \\ & \times \int \mathrm{d}^{2-\epsilon} K \frac{1}{K^2-\mathrm{i}\eta} (\mathrm{e}^{\mathrm{i}T((K^2-\mathrm{i}\eta)/k_-)} - 1) \\ & \times \frac{1}{(p-k)_-} \{\mathrm{e}^{-\mathrm{i}(p-k)_- L} - 1 + \mathrm{e}^{-\mathrm{i}p_- L}(\mathrm{e}^{\mathrm{i}(p-k)_- L} - 1)\} \\ & - \mathrm{i}\pi \int_0^{\infty} \mathrm{d}k_- \int \mathrm{d}^{2-\epsilon} K \frac{1}{K^2-\mathrm{i}\eta} (1 - \mathrm{e}^{-\mathrm{i}T(K^2-\mathrm{i}\eta)/k_-}) \\ & \times \frac{1}{(p-k)_-} \\ & \times \{\mathrm{e}^{-\mathrm{i}(p-k)_- L} - 1 + \mathrm{e}^{-\mathrm{i}p_- L}(\mathrm{e}^{\mathrm{i}(p-k)_- L} - 1)\}. \end{aligned} \tag{A13}$$

In the case of the lightlike Wilson loop we can omit the tadpoles in K^2 of the form

$$\int \mathrm{d}^{2-\epsilon} K \frac{1}{K^2-\mathrm{i}\eta} f(k_-, p_-) = 0. \tag{A14}$$

This step is not permitted for the spacelike or timelike lines (we explain why in Appendix C). Using the integral

$$\begin{aligned} T &= \int \mathrm{d}^{2-\epsilon} K \frac{1}{K^2-\mathrm{i}\eta} \mathrm{e}^{-\mathrm{i}T((K^2-\mathrm{i}\eta)/k_-)} \\ &= -\frac{2}{\epsilon} \pi^{1-(\epsilon/2)} \left(\frac{T}{k_-}\right)^{\epsilon/2} \mathrm{e}^{\mathrm{i}\pi\epsilon/4}, \end{aligned} \tag{A15}$$

and evaluating the remaining k_- integrals, we obtain

$$\begin{aligned} E = {} & \frac{2}{\epsilon} \mathrm{i}\pi^{2-(\epsilon/2)} \mathrm{e}^{\mathrm{i}\pi\epsilon/4} T^{\epsilon/2} {p_-}^{-\epsilon/2} \\ & \times \left\{ \frac{2}{\epsilon} (\mathrm{e}^{-\mathrm{i}Tp_+} - 1)(\mathrm{e}^{-\mathrm{i}p_- L} + 1) \right. \\ & + (\mathrm{e}^{-\mathrm{i}Tp_+} - 1) \\ & \times [(\mathrm{e}^{-\mathrm{i}p_- L} + 1)\mathrm{ci}(p_- L) + \mathrm{i}(\mathrm{e}^{-\mathrm{i}p_- L} - 1)\mathrm{si}(p_- L)] \\ & \left. - \mathrm{i}\pi(\mathrm{e}^{-\mathrm{i}p_- L} - 1) \right\}. \end{aligned} \tag{A16}$$

The non-capitalized ci and si functions are integrated cosine and sine commonly defined in the literature. The last integral is

$$\begin{aligned} F = {} & \int \mathrm{d}^n k \frac{1}{(p-k)^2 k_+} (\mathrm{e}^{-\mathrm{i}Tk_+} - \mathrm{e}^{-\mathrm{i}T(p-k)_+}) \\ & \times \frac{1}{(p-k)_-} (\mathrm{e}^{-\mathrm{i}k_- L} - 1)(1 - \mathrm{e}^{-\mathrm{i}(p-k)_- L}). \end{aligned} \tag{A17}$$

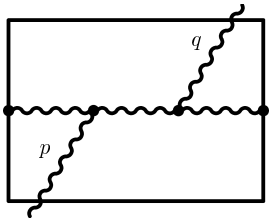

Fig. 19. The graph with two 3-gluon vertices which in the Feynman gauge contains no UV divergences. The same graph in the M–L gauge contains double divergences and single divergences with non-local Ci and Si functions

We use the same methods as for the integral E, but here the auxiliary formula is

$$\begin{aligned} & \int \mathrm{d}^{2-\epsilon} K \frac{1}{p_+ + \dfrac{K^2-\mathrm{i}\eta}{k_-}} \mathrm{e}^{-\mathrm{i}T(p_+ + (K^2-\mathrm{i}\eta)/k_-)} \\ & \quad = -\pi^{1-(\epsilon/2)} {k_-}^{1-(\epsilon/2)} \mathrm{Ei}(-\mathrm{i}Tp_+) \\ & \quad = -\pi^{1-(\epsilon/2)} {k_-}^{1-(\epsilon/2)} [\mathrm{ci}(p_+ T) - \mathrm{isi}(p_+ T)]; \end{aligned} \tag{A18}$$

we get

$$\begin{aligned} F = {} & -\mathrm{i}\pi^{2-(\epsilon/2)} \Gamma\left(\frac{\epsilon}{2}\right) (-p_+ p_- - \mathrm{i}\eta)^{-\epsilon/2} (\mathrm{e}^{-\mathrm{i}Tp_+} - 1) \\ & \times \{(\mathrm{e}^{-\mathrm{i}p_- L} + 1)\mathrm{Ci}(p_- L) + \mathrm{i}(\mathrm{e}^{-\mathrm{i}p_- L} - 1)\mathrm{Si}(p_- L)\} \\ & + \mathrm{i}\pi^{2-(\epsilon/2)} \Gamma\left(-\frac{\epsilon}{2}\right) L^{\epsilon/2} (\mathrm{e}^{-\mathrm{i}p_- L} + 1) \\ & \times \left\{ (\mathrm{e}^{-\mathrm{i}Tp_+} - 1) \left[\mathrm{ci}(p_+ T) + \frac{2}{\epsilon} {p_+}^{-\epsilon/2} - \gamma \right] \right. \\ & \left. + \mathrm{i}(\mathrm{e}^{-\mathrm{i}Tp_+} + 1)\mathrm{si}(p_+ T) + \mathrm{i}\pi \mathrm{e}^{-\mathrm{i}Tp_+} \right\} \\ & + \mathrm{i}\pi^{2-(\epsilon/2)} L^{\epsilon/2} {p_+}^{-\epsilon/2} (\mathrm{e}^{-\mathrm{i}Tp_+} + 1)(\mathrm{e}^{-\mathrm{i}p_- L} - 1) \\ & \times \frac{\mathrm{i}\pi}{\epsilon}. \end{aligned} \tag{A19}$$

The sum of the pole parts in $Z \cdot P$ is

$$Z \cdot P = Y + (E + F) = 0; \tag{A20}$$

hence there are no UV divergences in the transverse momentum P_β.

Appendix B

As an example of the complications caused by using the M–L gauge, let us take the diagram shown in Fig. 19 which in the Feynman gauge contains no ultra-violet divergences. In the M–L gauge the UV divergent part of this graph is

$$\begin{aligned} G_{\beta\rho} = {} & -2g^4 C_\mathrm{G} \mathrm{Tr}(t_b t_d) n_\beta n_\rho \pi^{2-(\epsilon/2)} (2\pi)^{-n} \\ & \times \left\{ \frac{8}{\epsilon^2} \frac{1}{q_+ p_+} \mathrm{e}^{-\mathrm{i}Tq_+} (\mathrm{e}^{-\mathrm{i}Tp_+} - 1)(\mathrm{e}^{-\mathrm{i}r_- L} + 1) \right. \\ & \left. - \frac{8}{\epsilon^2} \frac{1}{q_+ r_+} (\mathrm{e}^{-\mathrm{i}\mathrm{Tr}_+} - 1)(\mathrm{e}^{-\mathrm{i}r_- L} + 1) \right. \end{aligned}$$

$$
\begin{aligned}
&+\frac{2}{\epsilon}\frac{1}{q_+p_+}\mathrm{e}^{-\mathrm{i}Tq_+}(\mathrm{e}^{-\mathrm{i}Tp_+}-1)\\
&\times[(\mathrm{e}^{-\mathrm{i}r_-L}+1)(\mathrm{Ci}(r_-L)+2\ln(TL\mu^2)+\mathrm{i}\pi+2\gamma)\\
&+\mathrm{i}(\mathrm{e}^{-\mathrm{i}r_-L}-1)\mathrm{Si}(r_-L)]\\
&-\frac{2}{\epsilon}\frac{1}{q_+r_+}(\mathrm{e}^{-\mathrm{i}\mathrm{Tr}_+}-1)\\
&\times[(\mathrm{e}^{-\mathrm{i}r_-L}+1)(\mathrm{Ci}(r_-L)+2\ln(TL\mu^2)+\mathrm{i}\pi+2\gamma)\\
&+\mathrm{i}(\mathrm{e}^{-\mathrm{i}r_-L}-1)\mathrm{Si}(r_-L)]\\
&+\frac{2}{\epsilon}\frac{1}{q_+p_+}\mathrm{e}^{-\mathrm{i}Tq_+}\\
&\times[(\mathrm{e}^{-\mathrm{i}r_-L}+1)(\mathrm{Ci}(r_-L)-\mathrm{Ci}(q_-L)-\mathrm{Ci}(p_-L))\\
&+\mathrm{i}(\mathrm{e}^{-\mathrm{i}r_-L}-1)(\mathrm{Si}(r_-L)-\mathrm{Si}(q_-L)-\mathrm{Si}(p_-L))]\\
&-\frac{4}{\epsilon}\frac{1}{{r_+}^2}(\mathrm{e}^{-\mathrm{i}r_-L}+1)\\
&\times[(\mathrm{e}^{-\mathrm{i}\mathrm{Tr}_+}+1)\mathrm{Ci}(r_-L)+\mathrm{i}(\mathrm{e}^{-\mathrm{i}\mathrm{Tr}_+}-1)\mathrm{Si}(r_-L)]\}\\
&-\frac{8}{\epsilon}\frac{1}{r_+r_-}g_{\rho\beta}g^4C_\mathrm{G}\mathrm{Tr}(t_bt_d)\pi^{2-(\epsilon/2)}(2\pi)^{-n}\\
&\times\{(\mathrm{e}^{-\mathrm{i}\mathrm{Tr}_+}+1)\\
&\times[(\mathrm{e}^{-\mathrm{i}r_-L}+1)\mathrm{Ci}(r_-L)\\
&+\mathrm{i}(\mathrm{e}^{-\mathrm{i}r_-L}-1)(\mathrm{Si}(r_-L)-\pi)]+2\mathrm{i}\pi(\mathrm{e}^{-\mathrm{i}r_-L}-1)\}\\
&+\frac{4}{\epsilon}g^4C_\mathrm{G}\mathrm{Tr}(t_bt_d)n^*_\beta n_\rho\pi^{2-(\epsilon/2)}(2\pi)^{-n}\frac{1}{q_+r_-}\\
&\times\{(\mathrm{e}^{-\mathrm{i}Tq_+}-1)\\
&\times[(\mathrm{e}^{-\mathrm{i}r_-L}+1)(\mathrm{Ci}(p_-L)-\mathrm{Ci}(q_-L))\\
&+\mathrm{i}(\mathrm{e}^{-\mathrm{i}r_-L}-1)(\mathrm{Si}(p_-L)-\mathrm{Si}(q_-L)+\pi)]\\
&-(\mathrm{e}^{-\mathrm{i}r_-L}+1)\\
&\times[\mathrm{Ci}(r_-L)-\mathrm{Ci}(p_-L)+\mathrm{Ci}(q_-L)]\\
&-\mathrm{i}(\mathrm{e}^{-\mathrm{i}r_-L}-1)[\mathrm{Si}(r_-L)-\mathrm{Si}(p_-L)+\mathrm{Si}(q_-L)]\}\\
&-\frac{4}{\epsilon}g^4C_\mathrm{G}\mathrm{Tr}(t_bt_d)n^*_\rho n_\beta\pi^{2-(\epsilon/2)}(2\pi)^{-n}\frac{1}{p_+r_-}\mathrm{e}^{-\mathrm{i}Tq_+}\\
&\times\{(\mathrm{e}^{-\mathrm{i}Tp_+}-1)[(\mathrm{e}^{-\mathrm{i}r_-L}+1)\mathrm{Ci}(r_-L)\\
&+\mathrm{i}(\mathrm{e}^{-\mathrm{i}r_-L}-1)(\mathrm{Si}(r_-L)-\pi)]\\
&+(\mathrm{e}^{-\mathrm{i}r_-L}+1)[\mathrm{Ci}(p_-L)-\mathrm{Ci}(q_-L)+\mathrm{Ci}(r_-L)]\\
&+\mathrm{i}(\mathrm{e}^{-\mathrm{i}r_-L}-1)[\mathrm{Si}(p_-L)-\mathrm{Si}(q_-L)+\mathrm{Si}(r_-L)]\}.
\end{aligned}
\tag{B1}
$$

Appendix C

In the case of Wilson loops with spacelike and/or timelike lines strict application of dimensional regularization is not possible. As an example let us take the self-energy type of graph in the triangle Wilson loop with one spacelike[1] and two lightlike sides shown in Fig. 20.

$$
W_{\beta\rho}=C_{\beta\rho}\int\mathrm{d}^nk\frac{1}{k^2+\mathrm{i}\eta}\frac{k_-}{k_++\mathrm{i}\omega k_-}\frac{1}{k_3p_3}
$$

[1] This feature of the M–L prescription was noticed already in A. Andraši, hep-th 9411117, unpublished.

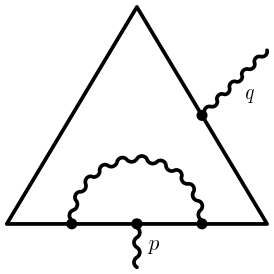

Fig. 20. The triangle Wilson operator. The base is along the spacelike vector v_β of length L, while the sides are along the lightlike vectors n and n^* of length $\frac{L}{2}$

$$
\begin{aligned}
&\times\left\{\frac{1}{(p-k)_3}\mathrm{e}^{-\mathrm{i}p_3L}(\mathrm{e}^{\mathrm{i}(p-k)_3L}-1)\right.\\
&\left.+\frac{1}{(p+k)_3}(\mathrm{e}^{-\mathrm{i}(p+k)_3L}-1)\right\}\\
&=C_{\beta\rho}W,
\end{aligned}
\tag{C1}
$$

where

$$
\begin{aligned}
C_{\beta\rho}=&-\mathrm{i}g^4v_\beta n_\rho\mathrm{Tr}(t_bt_d)(2\pi)^{-n}\frac{1}{q_+}\\
&\times(\mathrm{e}^{\mathrm{i}q_+L/2}-1)\mathrm{e}^{-\mathrm{i}q_-L/2}.
\end{aligned}
\tag{C2}
$$

There are two poles in the upper half complex k_0 plane.

(a)

$$
\begin{aligned}
k^2+\mathrm{i}\eta&=0,\\
k_0&=-k+\mathrm{i}\eta.
\end{aligned}
$$

(b)

$$
\begin{aligned}
k_++\mathrm{i}\omega k_-&=0,\\
k_0&=-k_3+2\mathrm{i}\omega k_3\theta(k_3).
\end{aligned}
\tag{C3}
$$

Let us take the first part of W with the $1/(p-k)_3$ denominator. After the k_0 integration it gives

$$
\begin{aligned}
W_1=&\,2\mathrm{i}\pi\mathrm{e}^{-\mathrm{i}p_3L}\int\mathrm{d}k_3\mathrm{d}^{2-\epsilon}K\frac{1}{2k}\frac{k+k_3}{k-k_3+\mathrm{i}\omega(k+k_3)}\\
&\times\frac{1}{k_3p_3(p-k)_3}\\
&\times\{\cos(p-k)_3L-1+\mathrm{i}\sin(p-k)_3L\}\\
&+2\mathrm{i}\pi\mathrm{e}^{-\mathrm{i}p_3L}\int_0^\infty\mathrm{d}k_3\int\mathrm{d}^{2-\epsilon}K\frac{2k_3}{K^2+4\mathrm{i}\omega k_3^2-\mathrm{i}\eta}\\
&\times\frac{1}{k_3p_3(p-k)_3}\\
&\times\{\cos(p-k)_3L-1+\mathrm{i}\sin(p-k)_3L\}.
\end{aligned}
\tag{C4}
$$

Naively, one would strictly apply the rules of dimensional regularization and set the second integral to zero as a tadpole in the perpendicular momentum K. However, after the introduction of polar coordinates,

$$
k_3=k\cos\theta=kx,
$$

$$\mathrm{d}^{3-\epsilon}k = k^{2-\epsilon}\mathrm{d}k(1-x^2)^{-\epsilon/2}\mathrm{d}x\int \mathrm{d}\Phi,$$
$$\int \mathrm{d}\Phi = \frac{2\pi^{1-\epsilon/2}}{\Gamma\left(1-\frac{\epsilon}{2}\right)} \tag{C5}$$

and integration over k, the first integral leads to an integral which is not defined for any ϵ.

Therefore we have to keep ω in the integrand and it becomes a part of the gauge. We can choose two ways. Either we evaluate integrals separately in terms of the spurious, "ambiguous" terms of the form $\omega^{-\epsilon/2}\epsilon^{-2}$ dictated by the tadpole

$$W^{\mathrm{T}} = \int \mathrm{d}^{2-\epsilon}K\frac{1}{K^2+4\mathrm{i}\omega k_3^2-\mathrm{i}\eta}$$
$$= \pi^{1-(\epsilon/2)}\Gamma\left(\frac{\epsilon}{2}\right)\omega^{-\epsilon/2}2^{-\epsilon}\mathrm{e}^{-\mathrm{i}\pi\epsilon/4}k_3^{-\epsilon}, \tag{C6}$$

or we transform the tadpole into polar coordinates

$$W^{\mathrm{T}} = \int_0^\infty \mathrm{d}k k^{-\epsilon}\int_0^1 \mathrm{d}x(1-x^2)^{-\epsilon/2}$$
$$\times \frac{1}{1-x^2+4\mathrm{i}\omega x^2}\int \mathrm{d}\Phi, \tag{C7}$$

and sum it up with the first integral in (C4) leading to

$$W_1 = -\mathrm{i}\pi\mathrm{e}^{-\mathrm{i}p_3L}p_3^{-1-\epsilon}$$
$$\times [\mathrm{ci}(p_3L)+\frac{1}{\epsilon}+\mathrm{i}\mathrm{si}(p_3L)+\mathrm{i}\pi]$$
$$\times \int \mathrm{d}\Phi\int_0^1 \mathrm{d}x(1-x^2)^{-\epsilon/2}x^{\epsilon-2}$$
$$\times \left[\frac{2(1+x^2)}{1-x^2+2\mathrm{i}\omega(1+x^2)}-\frac{4x}{1-x^2+4\mathrm{i}\omega x^2}\right]$$
$$+ (\mathrm{i}\pi)^2\mathrm{e}^{-\mathrm{i}p_3L}p_3^{-1-\epsilon}\int_0^1 \mathrm{d}x(1-x^2)^{-\epsilon/2}x^{\epsilon-2}$$
$$\times \frac{1-x}{1+x+\mathrm{i}\omega(1-x)}\int \mathrm{d}\Phi. \tag{C8}$$

We notice how crucial the contribution from the tadpole

$$-\frac{4x}{1-x^2+4\mathrm{i}\omega x^2}$$

is for the regularization of the pole at $x=1$. Only after the addition of the tadpole we can set $\omega=0$ in (C8) and evaluate the integrals in the strip $1<\epsilon<4$. In the same way we evaluate the second part of (C1) with $1/(p+k)_3$ denominator.[2]

Thus we obtain the result for (C1):

$$W_{\beta\rho} = -C_{\beta\rho}\frac{4\mathrm{i}\pi^{2-(\epsilon/2)}}{\Gamma\left(1-\frac{\epsilon}{2}\right)}p_3^{-1-\epsilon}2^{-\epsilon}\left[\frac{2}{\epsilon}+1\right]$$
$$\times\left\{(\mathrm{e}^{-\mathrm{i}p_3L}-1)\left(\mathrm{ci}(p_3L)+\frac{1}{\epsilon}\right)\right.$$
$$\left.+\ \mathrm{i}(\mathrm{e}^{-\mathrm{i}p_3L}+1)\left(\mathrm{si}(p_3L)+\frac{\pi}{2}\right)\right\}. \tag{C9}$$

This graph in the Feynman gauge contains only simple single poles. Hence, the funny non-local sine and cosine divergences and the double pole are caused by the choice of the M–L gauge, not the lightlike sides of the loop.

References

1. A. Andraši, J.C. Taylor, Nucl. Phys. B **516**, 417 (1998)
2. V.S. Dotsenko, S.N. Vergeles, Nucl. Phys. B **169**, 527 (1980)
3. R. Brandt, F. Neri, Masa-aki Sato, Phys. Rev. D **24**, 879 (1981)
4. G. Leibbrandt, Phys. Rev. D **29**, 699 (1984)
5. J.G.M. Gatheral, Phys. Lett. B **133**, 90 (1983)
6. J. Frenkel, J.C. Taylor, Nucl. Phys. B **246**, 231 (1984)
7. S. Mandelstam, Nucl. Phys. B **213**, 149 (1983)
8. A. Andraši, G. Leibbrandt, S.L. Nyeo, Nucl. Phys. B **276**, 445 (1986)
9. A. Andraši, J.C. Taylor, Nucl. Phys. B **302**, 123 (1988)
10. Physical and nonstandard gauges, Proceedings, Vienna, Austria 1989, edited by P. Gaigg, W. Kummer, M. Schweda

[2] Let us mention that the change of variable k_3 into $-k_3$ in the second part of (C1) is not permitted as it creates the pole in k_3.